Shake Test Results and Dynamic Calibration Efforts for the Large Rotor Test Apparatus

Carl Russell
Carl.R.Russell@nasa.gov
Aerospace Engineer, Rotorcraft Aeromechanics
NASA Ames Research Center
Moffett Field, CA

ABSTRACT

Prior to the full-scale wind tunnel test of the UH-60A Airloads rotor, a shake test was completed on the Large Rotor Test Apparatus. The goal of the shake test was to characterize the oscillatory response of the test rig and provide a dynamic calibration of the balance to accurately measure vibratory hub loads. This paper provides a summary of the shake test results, including balance, shaft bending gauge, and accelerometer measurements. Sensitivity to hub mass and angle of attack were investigated during the shake test. Hub mass was found to have an important impact on the vibratory forces and moments measured at the balance, especially near the UH-60A 4/rev frequency. Comparisons were made between the accelerometer data and an existing finite-element model, showing agreement on mode shapes, but not on natural frequencies. Finally, the results of a simple dynamic calibration are presented, showing the effects of changes in hub mass. The results show that the shake test data can be used to correct in-plane loads measurements up to 10 Hz and normal loads up to 30 Hz.

NOMENCLATURE

FEA	Finite Element Analysis
FRF	Frequency Response Function
LRTA	Large Rotor Test Apparatus
NFAC	National Full-Scale Aerodynamics Complex
RTA	Rotor Test Apparatus
α	Shaft angle of attack, positive aft, deg
C_T/σ	Thrust coefficient divided by solidity
F_{in}	Measured input force, lb
F_{out}	Measured output force, lb
N	Rotor harmonic number

INTRODUCTION

A shake test of the Large Rotor Test Apparatus (LRTA) was performed in an effort to enhance NASA's capability to measure dynamic hub loads for full-scale rotor tests. This paper documents the results of the shake test as well as efforts to calibrate the LRTA balance system to measure dynamic loads.

Oscillatory hub loads are the primary source of vibration in helicopters and other rotorcraft, leading to passenger discomfort and structural damage due to fatigue of aircraft components. The problem of both measuring and mitigating dynamic loads on rotorcraft airframes is not a new one; Ref. 1 provides a good overview of the history of the helicopter vibration problem. There are currently novel methods being developed to reduce rotor vibrations, and the experimental capability to measure dynamic loads on a full-scale rotor in a wind tunnel is key to understanding how well these methods work. NASA conducts full-scale wind tunnel tests on rotors using the LRTA and other test stands in the National Full-Scale Aerodynamics Complex (NFAC), so the capability to measure dynamic loads on these test stands is important.

In order to measure rotor forces on the LRTA, a balance system in the non-rotating frame is used. The forces at the balance can then be translated to the hub reference frame to measure rotor loads. A detailed description of the LRTA and its balance can be found in Ref. 2. Because the LRTA has its own dynamic response, measuring dynamic loads requires that the balance be calibrated to compensate for the natural frequencies of the test rig.

A similar dynamic calibration effort was performed on the Rotor Test Apparatus (RTA), and is described in Refs. 3-4. The RTA dynamic calibration effort investigated the effects of hub mass, pre-load, and rotation of the rotor shaft, and found that hub mass had the largest effect on the dynamic response. The dynamic calibration obtained for the RTA has been used with some success to measure dynamic hub loads on a full-scale rotor (Ref. 5). A shake test was performed on the LRTA in 2002 to determine ground resonance

Presented at the Fifth Decennial AHS Aeromechanics Specialists' Conference, San Francisco, CA, January 22-24, 2014.

frequencies, and some balance response data was acquired, but they were insufficient for dynamic calibration. The results of the 2002 shake test are detailed in Ref. 2.

For this test, a large shaker system was used to excite the LRTA at frequencies between 0 and 80 Hz. In addition to measurements from the balance and shaft bending gauges, the test rig was instrumented with accelerometers in order to measure the dynamic response of the entire LRTA. The purpose of collecting accelerometer measurements was to provide data that could be validated against a finite element model of the LRTA. Results of the shake test, as well as comparisons with a finite element analysis are presented in this paper. The ultimate goal is to use the data, along with mathematical models of the LRTA, to generate a dynamic calibration of the balance. This dynamic calibration could then potentially be used to correct measured oscillatory hub load data acquired during the UH-60A Airloads wind tunnel test, documented in Ref. 6. The results of a simple dynamic calibration, based on the frequency response functions (FRFs) derived from balance measurements and shaker load cell data, are presented at the end of this paper.

TEST DESCRIPTION

The shake test was carried out in the 40- by 80-foot test section of the NFAC prior to the UH-60A Airloads test. The LRTA was mounted on the NFAC's 8-ft struts with 33-in strut tips—the same as those used during the actual wind tunnel test. The UH-60A shaft extender and hub were mounted on the LRTA output shaft, and the "instrumentation hat" was mounted on top of the hub, but the rotor blades were not present. In order to facilitate shaking in the vertical direction, an adapter, weighing 384 lb, was fitted to the hub. This adapter is referred to as the "vertical shake plate" throughout this paper. Two hundred pounds of lead weights could also be attached to the vertical shake plate to help evaluate the sensitivity of the dynamic response to hub mass. The UH-60A hub and shaft extender together weigh approximately 800 lb, so the addition of the vertical shake plate and the lead weights represent a significant increase in weight at the hub. None of the bifilar weights were present for this test.

A hydraulic actuator system provided the shaking force. The point of application of in-plane oscillatory loads was the hub bifilar. The hydraulic actuator was backstopped against a 12,000 lb reaction mass, which was hung from the NFAC gantry crane and secured by guywires to the wind tunnel floor. A ±1,000 lb load cell was attached in series with the actuator and the reaction mass to measure the input loads. The input loads, consisting of a random signal with components from 0 to 80 Hz at ±800 lb, were generated at the actuator with a feedback control system. The test setup is shown in Figs. 1-3.

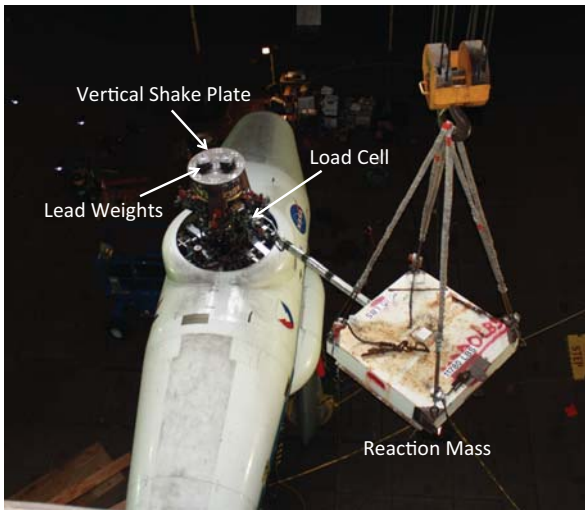

Figure 1. Shake test installation. In-plane shaking at 50° azimuth

Figure 2. Shake test installation. Vertical shaking on the hub centerline

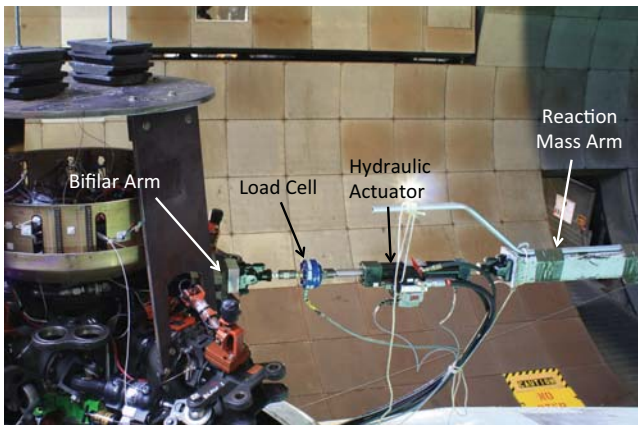

Figure 3. Close-up of load cell and actuator installation

The LRTA balance is made from a stainless steel ring that is 18" high by 49" in diameter. This ring has four machined cutouts leaving four symmetrically placed rectangular flexure posts separating an upper (metric side) and lower (non-metric side) ring. The lower ring sits on the LRTA transmission, and the upper ring supports the output shaft housing, which in turn supports the output shaft through two sets of bearings. Each of the flexure posts is instrumented with strain gauges measuring normal, axial, and side force. The forces measured at the flexures are typically combined to measure the overall rotor normal, axial, and side forces, along with pitch and roll moments at the hub. There are two sets of gauges on the balance, a primary and a backup set, for a total of 12 primary and 12 backup gauges. A schematic of the balance along with the sign conventions for balance forces and moments are shown in Fig. 4.

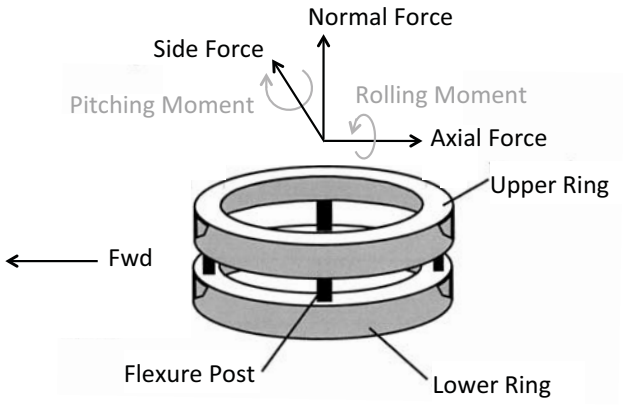

Figure 4. Schematic of LRTA rotor balance

The 12 primary balance gauges were used to collect loads data, with a separate data channel dedicated to each balance gauge. For the RTA dynamic calibration reported in Refs. 3 and 4, data was not collected for the individual balance gauges; instead, the gauge forces were resolved into balance forces and moments, which were then collected and analyzed. Unlike the RTA test, the intent with the current shake test of the LRTA was to collect the individual gauge measurements so that dynamic gauge interaction terms could be determined.

For this test, the UH-60A hub was supported by a two-part output shaft. The lower output shaft section is integral to the LRTA, and the upper part is a shaft extender identical to the one found on the UH-60A. The two shafts mate together via a spline interface. There are two bending strain gauges mounted on the LRTA output shaft and two on the UH-60A shaft extender that can be used together to measure in-plane loads and pitching and rolling moments at the hub. These bending gauges provided additional loads measurements for the shake test.

To help with validation of existing NASTRAN (Ref. 7) models of the LRTA, 48 accelerometers were placed at various locations on the test rig. The accelerometers were located on the LRTA chassis, as well as at the bases and tips of the support struts. Additional accelerometers were placed in the instrumentation hat and on the vertical shake plate. For in-plane shaking, an accelerometer was placed at the point of load application on the bifilar arm, parallel to the loading direction. The placement and directions of the accelerometers are shown in Fig. 5.

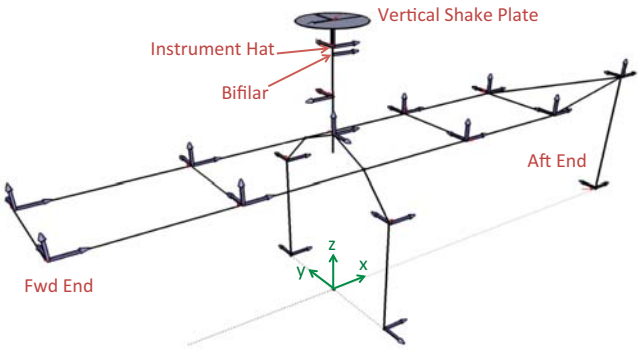

Figure 5. Shake test accelerometer locations

Data was collected simultaneously for the load cell, 48 accelerometers, 12 balance gauges, and 4 shaft bending gauges with a dynamic signal analyzer. The analyzer calculated and recorded frequency response functions and coherence for all channels over a frequency range of 0 to 80 Hz, with a spectral resolution of 0.1 Hz. The FRFs for the balance and shaft bending gauges were recorded in volts out per pound in, and then converted to engineering units. The accelerometer FRFs were recorded in *g*'s out per pound in.

The test matrix is given in Table 1. In-plane loads were applied at four azimuths to determine the response of the LRTA to different combinations of side and axial forces. Vertical loads were applied along the hub axis to obtain the pure normal load response. Off-center vertical loads were applied at three azimuthal locations and a radius of 15 inches from the hub axis to determine the response to pitch and roll moments. Note that only five forces and moments were investigated for this study; none of the loading scenarios included yaw moments.

The majority of testing was performed with the vertical shake plate attached to the hub and with the LRTA at zero degrees pitch. Two additional runs were performed at the end of the test with the shake plate removed to determine its effect on the frequency response. The effect of angle of attack was also considered, and a run was performed with the LRTA at an alpha of -10° (LRTA nose down).

Table 1. Shake test matrix. Shaking direction is indicated as in-plane or vertical along with the azimuth of shake application.

Configuration	In-Plane Shake Azimuth (°)	Vertical Shake Location (°)
With shake plate and 200 lb mass	0, 270, 315, 50	Center, 0, 270, 315
With shake plate and no 200 lb mass	0, 270, 315, 50	Center, 0, 270, 315
With shake plate and LRTA 10° nose down	270	—
Without shake plate	0, 270	—

SHAKE TEST RESULTS

Results are first presented for the balance gauges and shaft bending gauges. The accelerometer data is presented in the following section.

Balance Results

Results are presented here for a subset of the loading scenarios given in Table 1. Figures 6-8 show the effect of hub mass on the magnitude of the frequency response measured at the balance. For each of the three primary force measurement directions (axial, side, and normal) the forces measured by the four balance gauges were summed to obtain the total force. Balance gauge interactions were not considered for the presentation of these initial results. Note that the three plots use the same scale on the y-axis. This is to emphasize the difference in behavior of the LRTA with respect to in-plane versus vertical shaking. The N per rev scale on the top of Figs. 6-8 is based on the nominal operating speed (258 RPM) of the UH-60A main rotor. Frequency response functions were calculated for frequencies up to 80 Hz. In general, it appears that the shaker did not generate enough energy to excite the LRTA above 40 Hz, so the plots are truncated at 8/rev, or 34.4 Hz.

As Figs. 6 and 7 clearly show, hub mass has a large effect on the measurement of in-plane loads. There are two strong modes in the axial direction at 13.0 and 17.4 Hz when both the vertical shake plate and the additional 200 lb of mass are present. With the 200 lb removed, a single mode appears at 16.8 Hz, and when the 384-lb vertical shake plate is removed, this mode moves to 25.8 Hz. The results in Fig. 7 for shaking in the y-direction show similar behavior, but the natural frequencies are different. Note that the frequency of these inconsistent modes in both the x- and y- directions is near 4/rev of the UH-60A rotor.

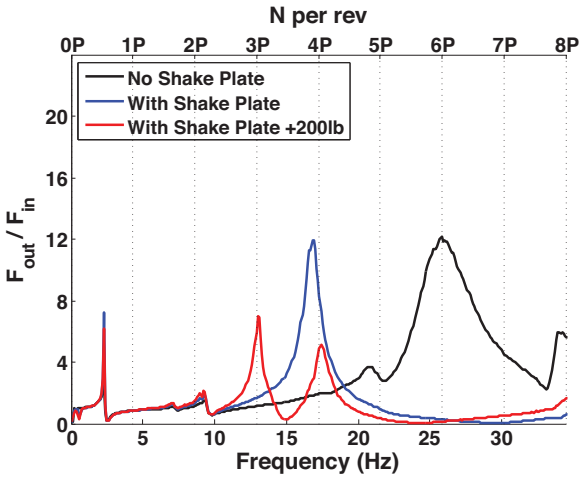

Figure 6. Frequency response magnitude – axial force, 0° in-plane shaking

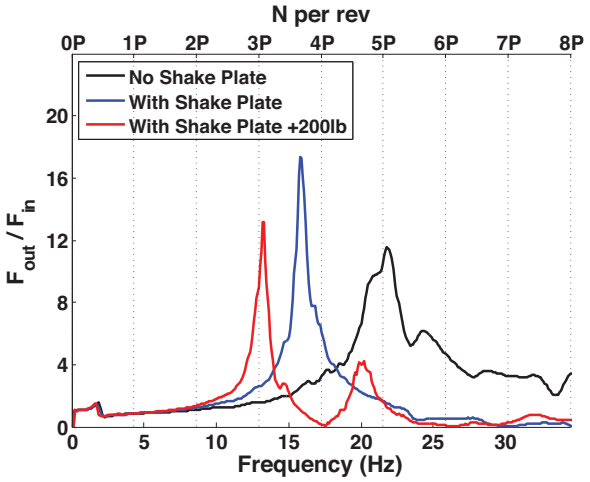

Figure 7. Frequency response magnitude – side force, 270° in-plane shaking

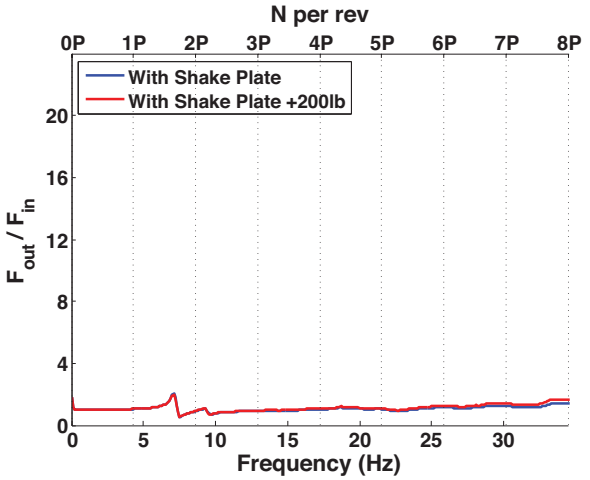

Figure 8. Frequency response magnitude – normal force, vertical on-center shaking

The accelerometer data, presented later in this paper, was used to identify the mode shapes at various resonant frequencies. The accelerometer data shows that bending of the LRTA output shaft is the cause of the mass-dependent mode near 4/rev. The variation in hub mass is apparently enough to cause the large variations observed in natural frequency and magnitude. It is unclear why the shaft-bending mode splits into two distinct peaks when the additional 200 pounds of lead weights are added on top of the vertical shake plate.

A simplified calculation was made using Rayleigh's Method (Ref. 8) to help determine how the natural frequency of a shaft-bending mode might vary with hub mass. In making these calculations, the upper and lower bearings on the rotor shaft were assumed to form rigid constraints, and a quadratic mode shape was assumed. The resulting calculations gave a frequency of 12.6 Hz for a hub weight of 800 lb. When the assumed hub weight was increased to 1,000 lb, the frequency dropped to 11.4 Hz. While not identical to the frequencies observed in the shake test, this result confirms that the different hub masses used for this test could cause the observed changes in the shaft-bending mode natural frequency.

In addition to the shaft-bending modes, there are modes that do not change in frequency with hub mass, though they do change in magnitude. The most prominent example of this is the strong axial mode at 2.3 Hz. This is a known mode that is due to bending of the wind tunnel support struts. There are two additional modes at 7.1 and 9.2 Hz that have not been previously documented. The accelerometer data shows that bending of the LRTA chassis is the cause of these modes. The variations observed in the chassis-bending modes appear to be due to superposition with the shaft-bending mode, rather than a global change in the mode shape. The magnitude of the strut-bending mode also varies between hub configurations, but the peak in the FRF is so sharp that this discrepancy is likely due to the frequency resolution of 0.1 Hz. The variations in the FRFs below 1 Hz appear to be artifacts of the signal analysis.

In Fig. 8, the response of the LRTA to vertical shaking shows minimal variation with changes in hub mass. There are only two mass configurations for normal force, because the vertical shake plate is necessary to apply loads in the z-direction. The response in the z-direction is mostly flat, with the only observable modes at 7.1 and 9.2 Hz due to chassis bending. Hub mass has little to no effect on the total normal force frequency response, but the shaft-bending mode can, in fact, be excited by normal force excitation. Figure 9 shows the response of the individual normal force gauges to vertical shaking on the hub axis. The balance gauge locations are indicated in Fig. 9 by their azimuth (e.g., NF180 is the normal force gauge at 180 degrees azimuth). Figure 9 shows that the forward-aft shaft-bending mode is present, but the gauge normal forces for this mode are 180 degrees out of phase, so they cancel out upon summation.

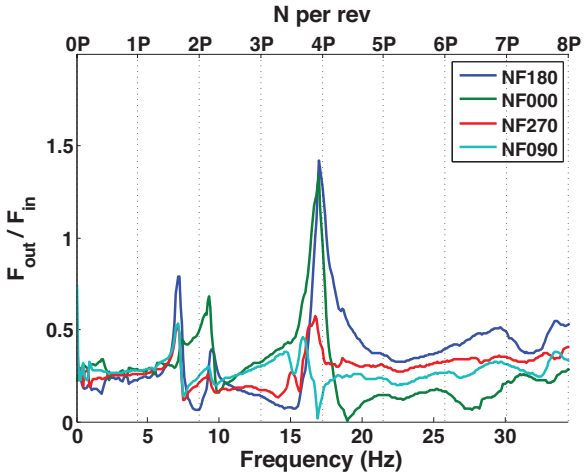

Figure 9. Frequency response magnitude – individual normal force gauge measurements, vertical on-center shaking, shake plate present without additional 200 lb

Cross-coupling with the shaft-bending mode is even more pronounced for in-plane loads between the x- and y-directions. Figure 10 shows the results for in-plane shaking in the axial direction, with response magnitude for both side and axial force. The blue line shows the same data as the blue line in Fig. 6: the axial force magnitude from axial shaking. The green line shows the response in the y-direction due to axial shaking. If there were no cross-coupling between side and axial forces and the experiment was executed perfectly (perfect alignment of the shake direction and 0 degrees azimuth), the side force response would be zero; however, near the resonant frequency of the shaft-bending mode, the output side force is nearly 3 times the input axial force. This result indicates that near the natural frequency of the shaft-bending mode, either the side and axial forces are strongly coupled, or the shaker was not perfectly aligned.

Figure 11 shows similar results to Fig. 10, except the results in Fig. 11 are for in-plane shaking at 270° azimuth. The blue line shows the same side force data as the blue line in Fig. 7. The green line shows the axial response to the input side force. The apparent cross-coupling isn't quite as prominent here as in Fig. 10, but is still present, further indicating that side and axial response may not be independent.

Another independent variable investigated during the shake test was angle of attack. All shake runs except for one were performed at 0 degrees alpha, with a single run at 10 degrees nose-down and shaking applied at 270 degrees azimuth. The results are shown in Fig. 12. The blue curve is the same as the blue curve in Fig. 7. The green curve shows the magnitude of the frequency response for α = -10°. Angle of

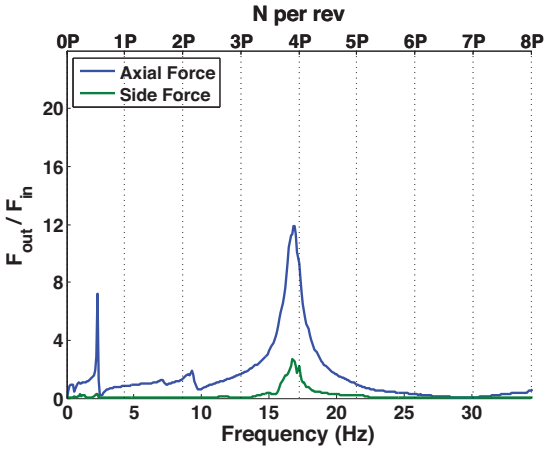

Figure 10. Frequency response magnitude – axial and side force for 0° in-plane shaking, shake plate present without additional 200 lb

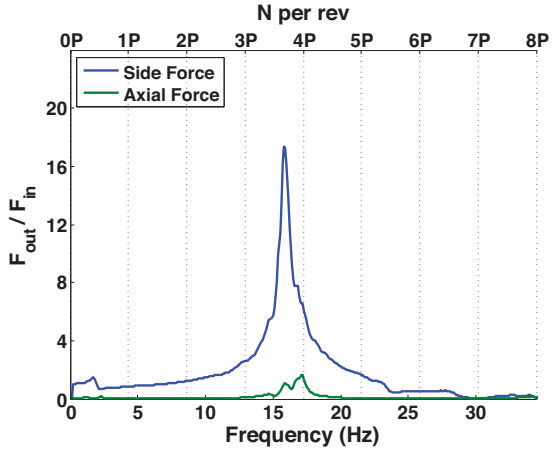

Figure 11. Frequency response magnitude – side and axial force for 270° in-plane shaking, shake plate present without additional 200 lb

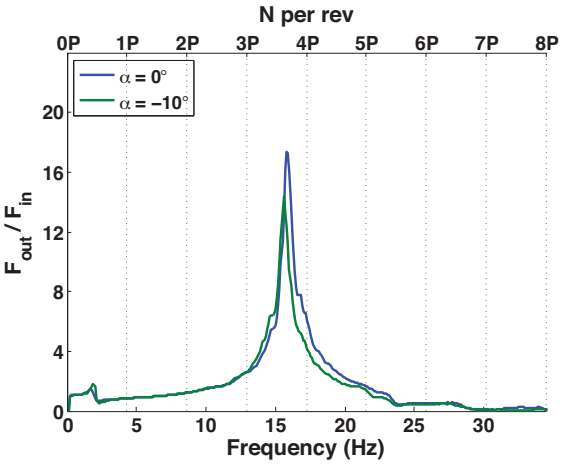

Figure 12. Frequency response magnitude – side force for 270° in-plane shaking at varied angle of attack, shake plate present without additional 200 lb

attack has almost no effect on the frequency response, except near the shaft-bending mode, where the frequency of the peak differs by 0.2 Hz, and the amplification factor differs by approximately 3. Since there was only a single run at α = -10°, it is difficult to draw definitive conclusions from the results shown in Fig. 12. The plot suggests that angle of attack has only a minor impact on the frequency response in the y-direction, especially compared with FRF changes due to variations in hub mass. The effect on the other two force directions and on moments is unknown. Results from the current NASTRAN model of the LRTA suggest that angle of attack could have a greater impact in the other shake directions, but this effect has not been experimentally verified.

Dynamic hub moments were applied by off-center vertical shaking. Once again, the shaft-bending mode dominates the balance-measured response near the 4/rev frequency. The lower frequency modes present in Figs. 6 and 7 do not appear in the moment measurements. Pitching and rolling moment response are shown in Figs. 13 and 14, respectively. Note that the frequencies of the observed modes are not necessarily identical to those shown in Figs. 6 and 7. For example, the blue curve in Fig. 13 shows a peak just below 4/rev, the same frequency as the peak of the blue curve in Fig. 6; however, the red curve in Fig. 13 shows a single peak at approximately 3.3/rev, while the corresponding red curve in Fig. 6 shows peaks at approximately 3/rev and 4/rev. The reason for this discrepancy has not been determined, but hub mass clearly has an impact on dynamic moments measured at the balance.

Shaft Bending Gauge Results

The individual measurements provided by the four shaft bending gauges were combined to calculate FRFs for in-plane forces and hub moments. Data for the shaft bending gauges was then compared against the results from the balance. Figures 15-17 show the balance and shaft bending gauge axial force with the three different hub configurations for 0° in-plane shaking. The blue curves in Figs. 15-17 show the same balance data as the black, blue, and red curves, respectively, in Fig. 6. The red curves in Figs. 15-17 show the corresponding results from the shaft bending gauges. In general, the balance results show good agreement with the shaft bending gauge results, especially for the shaft-bending mode. The agreement improves when the hub mass is higher. For the modes involving the entire LRTA chassis (modes near 2, 7, and 9 Hz), the shaft bending gauges show a small response, but it is weaker than the response measured at the balance.

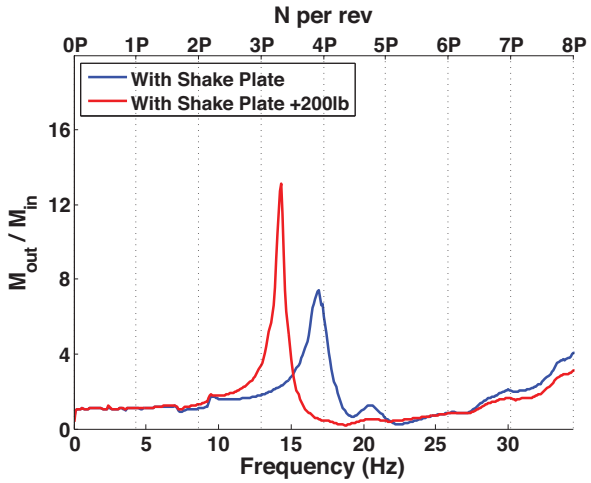

Figure 13. Frequency response magnitude – pitching moment for 0° vertical shaking

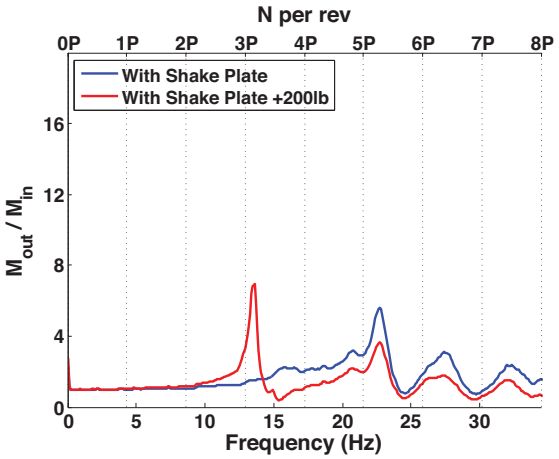

Figure 14. Frequency response magnitude – rolling moment for 270° vertical shaking

Comparisons were also made between the shaft bending gauges and the balance for hub moments. Figures 18 and 19 show the balance and bending gauge results for pitching moments applied by vertical shaking at 0° azimuth for the two different vertical shake plate configurations. The blue curves here show the same data as the curves in Fig. 13. The agreement between the two measurements is good. For this shake direction, the only observable mode for the pitching moment is the shaft-bending mode, and it is predicted with similar magnitude by the balance and the shaft bending gauges.

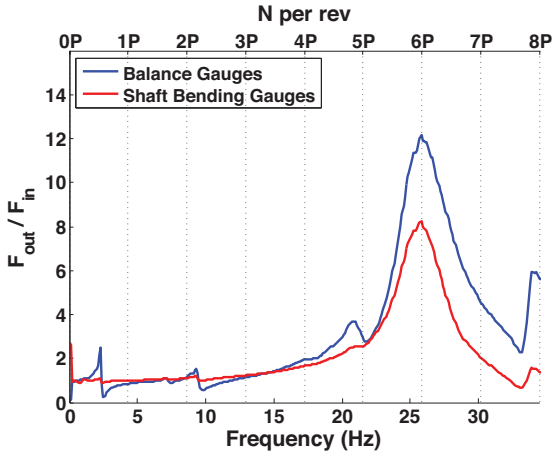

Figure 15. Comparing balance and bending gauges – axial force for 0° in-plane shaking, no vertical shake plate

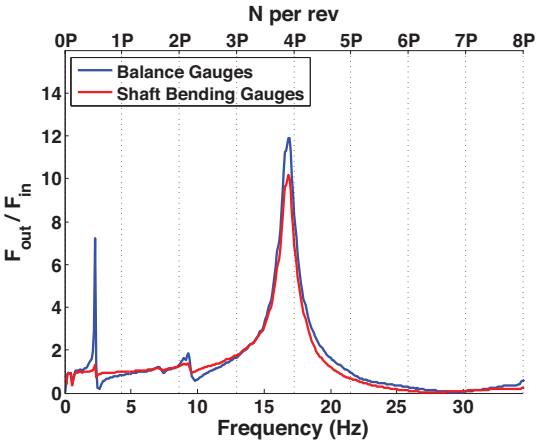

Figure 16. Comparing balance and bending gauges – axial force for 0° in-plane shaking, vertical shake plate present without additional mass

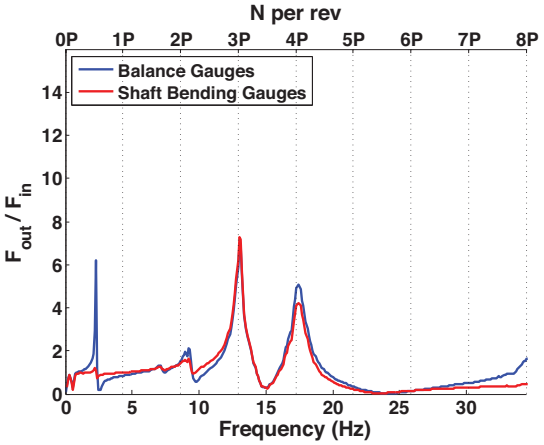

Figure 17. Comparing balance and bending gauges – axial force for 0° in-plane shaking, vertical shake plate present with additional 200 lb

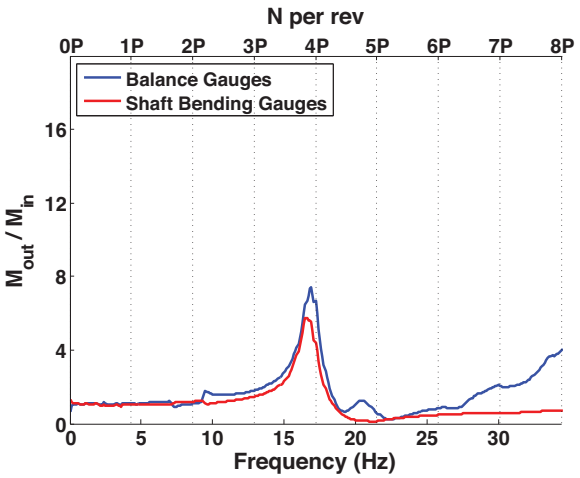

Figure 18. Comparing balance and bending gauges – pitching moment for vertical shaking at 0°, vertical shake plate present without additional mass

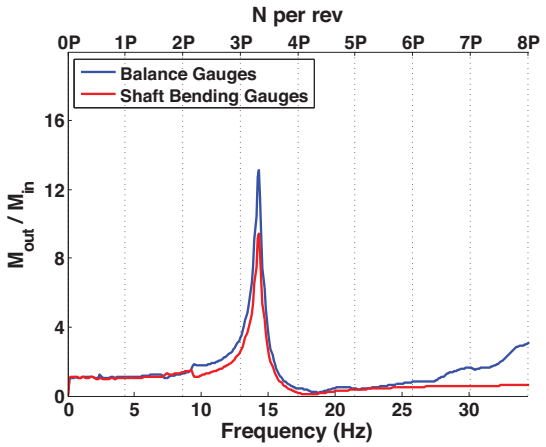

Figure 19. Comparing balance and bending gauges – pitching moment for vertical shaking at 0°, vertical shake plate present with additional 200 lb

Insights from the Balance and Bending Gauge Results

The results presented in the previous two sections show that changes in hub mass have a large effect on measurements of in-plane forces and pitch and roll moments on the LRTA. Normal force is largely unaffected by changes in hub mass. The ultimate goal of the shake test described here was a dynamic calibration of the LRTA balance. In order to generate this dynamic calibration, it is necessary to know the amplification factor for the frequency of interest. For the UH-60A, 4/rev is particularly important, but the 1/rev to 8/rev frequencies are also of interest.

Based on the results already presented, it would be exceedingly difficult, if not impossible, to create an accurate calibration over the entire frequency range of interest based on the shake test data alone. The peaks in the FRFs are so narrow, that a natural frequency change of even 0.5 Hz could easily change the amplification by a factor of two or more. A simple dynamic calibration has been performed, and the results, presented in a following section, show how changes in hub mass affect the resulting transfer functions. The presence of a shaft-bending mode that is both near the 4/rev frequency and is highly dependent on hub mass is, to say the least, problematic.

Accelerometer Results

An alternate approach that has been proposed for generating a dynamic calibration is to create a finite element analysis (FEA) model that can be tuned to replicate the behavior of the LRTA. Transfer functions would then be generated based on simulation results. Accelerometer mode shape and frequency data was used to compare the experimental results of the shake test with results from an existing NASTRAN model. This NASTRAN model includes the LRTA chassis, balance, support struts, and T-frame base. Six of the modes identified by analysis of the NASTRAN model are clearly visible in the shake test data.

The modes that are recognizable in both the NASTRAN model and the accelerometer data are identified in Table 2. Figure 20 shows a comparison between the NASTRAN mode shape (top image) and the corresponding accelerometer mode shape (bottom image) for mode number 3 listed in Table 2. The red dots on the lower image indicate the locations of the accelerometers. The gray or dotted lines show the un-deformed shape of the LRTA. Even though the mode shapes are similar, the frequencies are not identical. In general, the NASTRAN model over-predicts the frequency, and the amount of over-prediction increases with the frequency of the mode. The shake test frequencies in Table 2 are for the case where the vertical shake plate is present, but the additional 200 lb of lead weights are not. The balance force FRFs for the three principle shake directions are shown in Fig. 21 with the Table 2 mode numbers identified in red.

The accelerometer data shows that the modes involving motion of the entire LRTA are not affected by the mass of the hub. The modes that involve only motion of the hub and rotor shaft, however, are very sensitive to the mass placed on the hub. Modes 5 and 6 in Table 2 involve very little motion of any component except the rotor shaft and hub.

The NASTRAN model has not been tuned to match the accelerometer data, but the fact that several of the mode shapes approximately match is encouraging. To explore whether a FEA model of the LRTA could be tuned to match the behavior of the test rig, a 3-dimensional solid model was developed using the Creo mechanical design software suite (Ref. 9). Because the shaft-bending modes involve very little motion of the LRTA chassis, a simplified FEA model was used, including just the LRTA output shaft and UH-60A

shaft extender. The hub was modeled as a point mass. Changing the mass at the hub as well as adjusting the height of the hub above the top of the output shaft had a large effect on the first natural frequency observed. This result indicates that it would be possible to tune the FEA model to match the behavior of the LRTA; however, a calibration has not yet been generated using this method. This is a possible avenue for future research.

It may also be possible to directly measure rotor loads with accelerometer data. This method is detailed in Ref. 10, and relies on measuring the vibratory response of an entire airframe to applied loads. To measure rotor loads, the method would require placing accelerometers on the LRTA during wind tunnel testing, which was not the case for the Airloads wind tunnel test. With the accelerometer data already collected, though, this method could be useful for future wind tunnel tests.

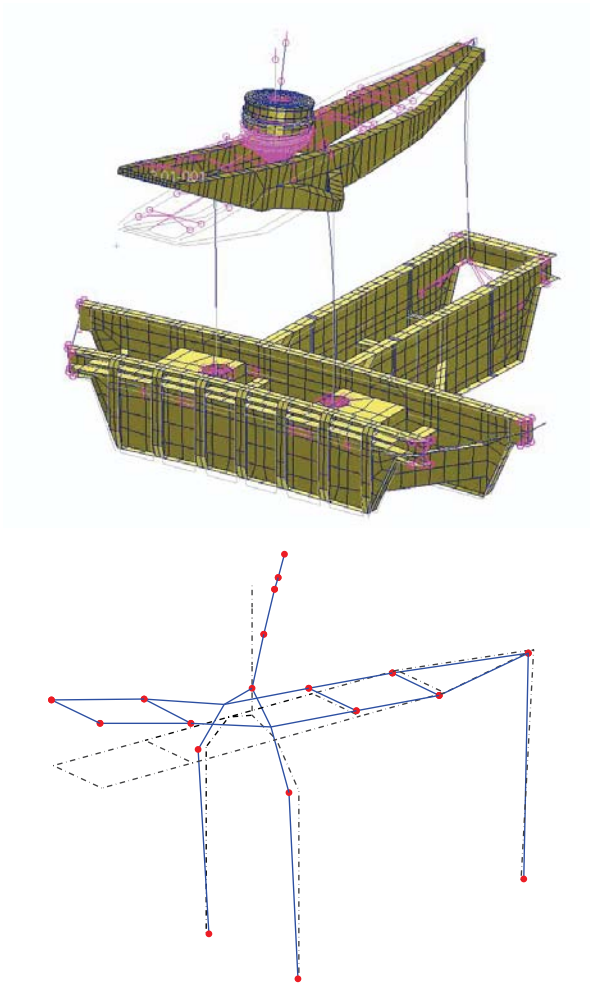

Figure 20. Comparison of NASTRAN model (top) and accelerometer data (bottom) mode shapes – Mode 3

Table 2. Modes and frequencies from both the NASTRAN model and the shake test

Mode Number	Mode Shape	NASTRAN Frequency (Hz)	Shake Test Frequency (Hz)
1	Lateral strut bending	2.4	1.7
2	Longitudinal strut bending	2.4	2.3
3	Chassis vertical bending	8.9	7.2
4	Chassis + T-frame vertical bending	13.4	9.3
5	Rotor shaft lateral bending	26.1	15.9
6	Rotor shaft longitudinal bending	29.9	16.9

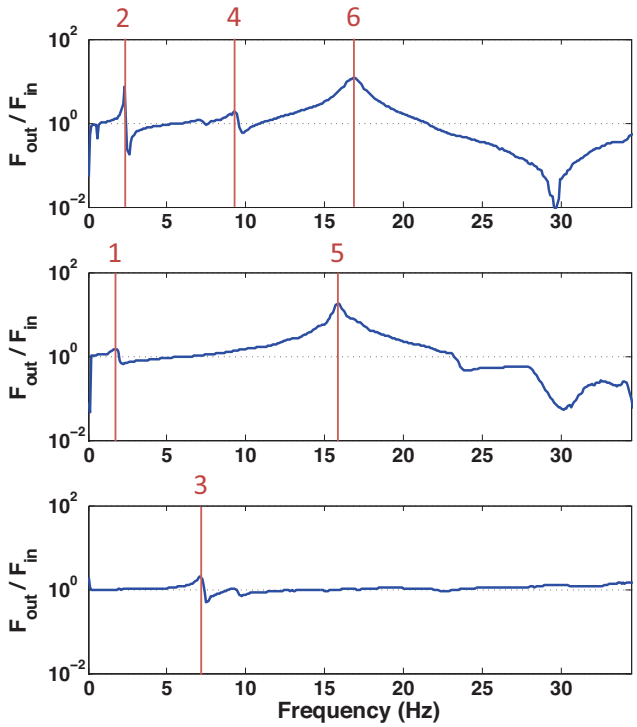

Figure 21. Mode identification for axial force, in-plane shaking at 0° (top); side force, in-plane shaking at 270° (middle); normal force, vertical shaking on-center (bottom). Note logarithmic scale on y-axis.

DYNAMIC CALIBRATION

A simple dynamic calibration has been attempted using the shake test data, and the results were used to reduce data taken during the recently completed UH-60A Airloads wind tunnel test. The calibration is very simple, and uses only one-dimensional transfer functions. To obtain the corrected hub forces, the uncorrected balance loads were multiplied by the inverse of the transfer functions shown in Figs. 6-8. In order to simplify the calculations, cross-coupling between lateral and longitudinal forces was not considered. As shown in the Balance Results section, this assumption may not be valid near 4/rev. Balance gauge interactions were not considered for these calculations. The data point chosen from the Airloads wind tunnel test is Run 52, Point 31, which was conducted at an advance ratio of 0.3, α of –4.2°, and C_T/σ of 0.09. Ref. 6 contains a summary of the Airloads wind tunnel test conditions. Rotor speed at this data point was 258 RPM, and the total measured steady thrust was 20,467 lb.

Figures 22-24 show the results for the first eight UH-60A rotor harmonics (4.3 Hz to 34.4 Hz) using three different calibrations, one for each of the hub configurations tested. The uncorrected loads are shown for comparison. Note that Figs. 22 and 23 use a logarithmic scale on the y-axis. The y-axis on Fig. 24 uses a linear scale. Neither the corrected, nor uncorrected in-plane loads measurements provide trustworthy results above 2/rev. As expected, the magnitude of the corrected oscillatory in-plane hub loads varies widely for the 3/rev harmonics and higher, depending on the calibration used. At 4/rev, the difference of 200 lb on the hub causes a difference of almost two orders of magnitude in the corrected side force. With the heaviest hub configuration, there is an antiresonance in the y-direction at 4/rev (see Fig. 7), causing a high amplification factor in the resulting calibration. Figures 22 and 23 make it clear that for in-plane loads, this balance calibration is only potentially useful for 1/rev and 2/rev. For normal loads, harmonics up to 7/rev can be measured with only minor differences between the calibrations.

During the Airloads test there were several slowed-rotor runs performed; for a full list of these test conditions, see Ref. 11. The 1-dimensional dynamic calibration was applied to a slowed-rotor run, and the results are shown in Figs. 25-27. The data represents Run 91, Point 50, which had the rotor turning at 40% of full speed. Alpha was 0° for this run, advance ratio was 0.7, and C_T/σ was 0.04. Total measured static thrust was 1,463 lb.

For the slowed-rotor measurements presented in Figs. 25-27, the different calibrations lead to more consistent results for the first 8 harmonics (1.7 Hz to 13.9 Hz) than for the full-speed example. The normal loads look especially good. For the most part, the corrected loads match the uncorrected

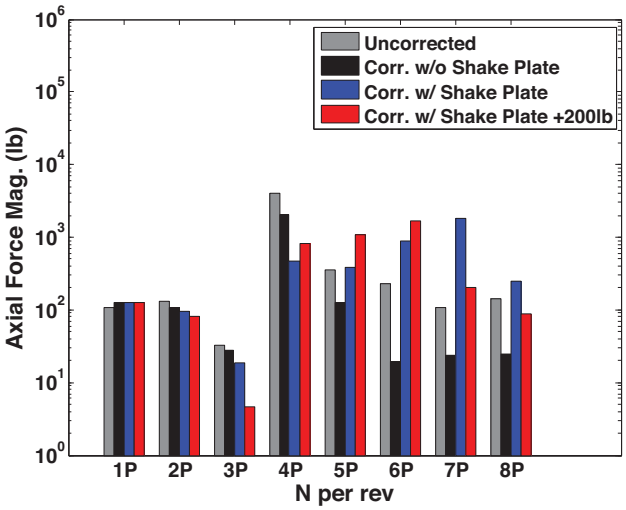

Figure 22. Axial loads for run 52, point 31

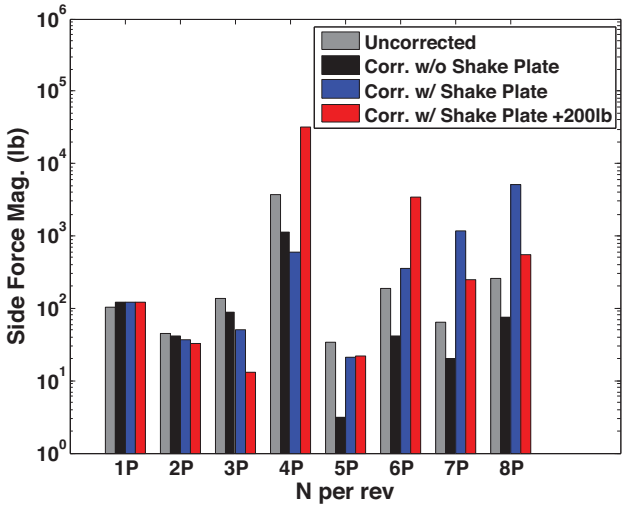

Figure 23. Side loads for run 52, point 31

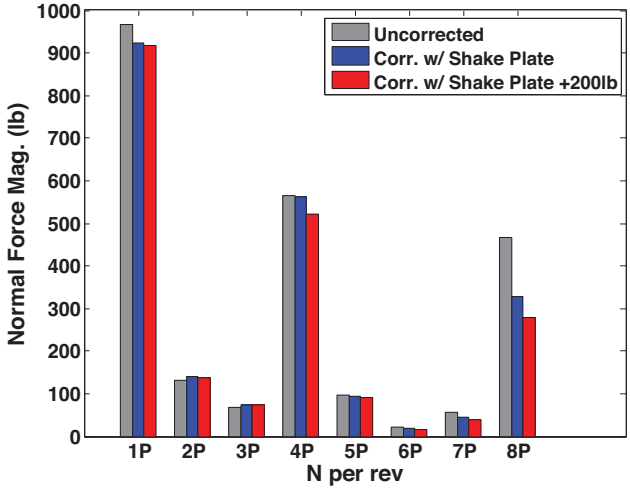

Figure 24. Normal loads for run 52, point 31

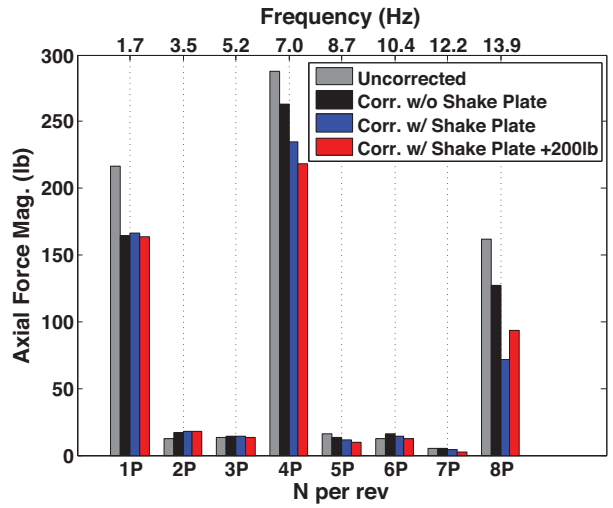

Figure 25. Axial loads for Run 91, Point 50

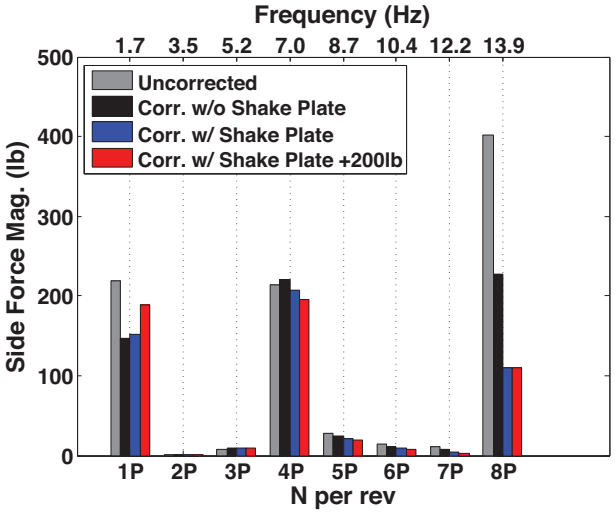

Figure 26. Side loads for Run 91, Point 50

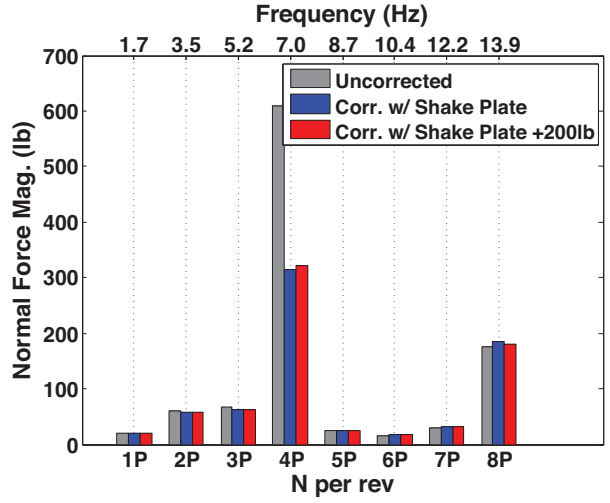

Figure 27. Normal loads for Run 91, Point 50

loads very well. At 4/rev, the chassis vertical bending mode (Mode 3 in Table 2) causes an amplification of approximately 2x, which is equally predicted by the two calibrations used. In-plane loads corrections are not as consistent across the different calibrations, especially at 4/rev and 8/rev. At 4/rev, the effect of the chassis-bending mode varies across the three hub configurations, due to the placement of the shaft-bending mode. The 8/rev frequency for this slowed-rotor case is close to the shaft-bending mode, so the loads measured with the different calibrations vary widely.

CONCLUSIONS

This paper presented the results of a shake test of the Large Rotor Test Apparatus, carried out in the 40- by 80-foot test section of the National Full-Scale Aerodynamics Complex. This test was executed prior to the UH-60A Airloads wind tunnel test with the intention of generating a dynamic calibration of the LRTA five-component rotor balance. In addition to the balance, frequency response data was collected for the shaft bending gauges and for accelerometers placed on the LRTA. Results for balance, bending gauges, and accelerometers were presented here. Finally, the results of a simple 1-dimensional dynamic calibration were presented, showing how the shake test data could be used to correct dynamic loads measurements from the Airloads wind tunnel test. Based on the results presented, the following conclusions can be drawn:

1. The shake test provided frequency response data for the LRTA for a variety of hub loading scenarios at frequencies up to approximately 35 Hz, or 8/rev for the UH-60A rotor.

2. At frequencies near 4/rev (17.2 Hz), the LRTA has a strong shaft-bending mode that is highly dependent on the mass of the hub. The variability of this mode makes determination of moments and in-plane loads at 3/rev (12.9 Hz) and higher difficult, if not impossible, if the dynamic calibration of the balance is based on the shake test data alone.

3. The normal loads measured at the balance are only minimally affected by hub mass. Normal loads up to 7/rev (30.1 Hz) can therefore be corrected based on the shake test balance data.

4. A balance calibration based on the shake test data can be used to correct dynamic loads at a broader range of harmonics for the slowed-rotor Airloads test runs, as long as the frequencies of interest are below approximately 10 Hz.

5. Accelerometer data provided mode shapes that correspond to an existing NASTRAN model of the

LRTA. Tuning the NASTRAN model to match the accelerometer data may provide another means of dynamic loads calibration.

ACKNOWLEDGEMENTS

Benton Lau planned and executed the LRTA shake test, and the author would like to gratefully acknowledge his contribution to the work presented here. Brandon Hagerty and Charlie Rogers were especially helpful in providing their recollections of the test to fill in the gaps. Finally, the author would like to thank Tom Norman for his guidance and advice throughout this effort.

REFERENCES

1. Harris, F. D., *Introduction to Autogyros, Helicopters, and other V/STOL Aircraft, Vol. 2: Helicopters*, NASA SP-2012-215959, Vol. 2, October 2012, pp. 315-435.

2. Norman, T., Shinoda, R., Kitaplioglu, C., Jacklin, S., and Sheikman, A., "Low-Speed Wind Tunnel Investigation of a Full-Scale UH-60 Rotor System," American Helicopter Society 58th Annual Forum, Montreal, Canada, June 11-13, 2002.

3. Peterson, R. and van Aken, J., "Dynamic Calibration of the NASA Ames Rotor Test Apparatus Steady/Dynamic Rotor Balance," NASA TM 110393, April 1996.

4. van Aken, J., Peterson, R., and Freedman, C., "Calibration Results of the NASA Ames Rotor Test Apparatus Steady/Dynamic Rotor Balance," American Helicopter Society Aeromechanics Specialists Conference, San Francisco, CA, January 19-21, 1994.

5. Wang, J., and van Aken, J., "Correlation of Vibratory Hub Loads for a Sikorsky Full-Scale Bearingless Main Rotor," American Helicopter Society 50th Annual Forum, Washington, D.C., May 11-13, 1994.

6. Norman, T., Shinoda, P., Peterson., Datta., "Full-Scale Wind Tunnel Test of the UH-60A Airloads Rotor," American Helicopter Society 67th Annual Forum, Virginia Beach, VA, May 3-5, 2011.

7. *MSC NASTRAN 2012 Quick Reference Guide*, MSC.Software Corporation, 2012.

8. Rao, S., *Mechanical Vibrations*, Pearson Education, Inc., New Jersey, 2004, pp. 631-632.

9. *PTC Creo® Simulate Data Sheet*, PTC, Inc., 2012.

10. Giansante, N., Jones, R., and Calapodas, N.J., "Determination of In-Flight Helicopter Loads," American Helicopter Society 37th Annual Forum, New Orleans, LA, May 1981.

11. Datta, A., Yeo, H., Norman, T., "Experimental Investigation and Fundamental Understanding of a Full-Scale Slowed Rotor at High Advance Ratios," *Journal of the American Helicopter Society*, 58, 022004 (2013), DOI: 10.4050/JAHS.58.022004.